

# Charge transfer in collisions of $C^{2+}$ ions with H atoms at low-keV energies: A possible bound state of $CH^{2+}$

J.-P. Gu, G. Hirsch, and R. J. Buenker

*Theoretische Chemie, Bergische Universität–Gesamthochschule Wuppertal, D-42097 Wuppertal, Germany*

M. Kimura

*School of Allied Health Sciences, Yamaguchi University, Ube, Yamaguchi 755, Japan  
and Institute of Space and Astronautical Science, Sagami-hara, Kanagawa 229, Japan*

C. M. Dutta and P. Nordlander

*Department of Physics and Rice Quantum Institute, Rice University, Houston, Texas 77251-1892*

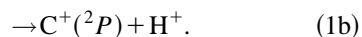
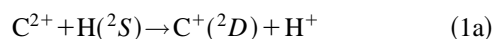
(Received 29 April 1997)

Electron capture in  $C^{2+}+H$  collisions is studied theoretically by using a semiclassical molecular representation with nine molecular states for the doublet manifold at collision energies above 10 eV. The *ab initio* potential curves and nonadiabatic coupling matrix elements for the  $CH^{2+}$  system are obtained from the multireference single- and double-excitation configuration interaction method. The adiabatic potential curves show no bound state for the  $1^2\Sigma^+$  state, but a very shallow well in the  $2^2\Sigma^+$  potential, suggesting a possibility of a bound state of  $CH^{2+}$ . The corresponding total and partial cross sections for charge transfer are found to be in a reasonable agreement with experiment in shape, but the present magnitude is found to be larger by nearly a factor of 2 at the high-energy end. [S1050-2947(98)09606-1]

PACS number(s): 34.10.+x, 34.70.+e, 34.20.-b

## I. INTRODUCTION

Knowledge of charge transfer from heavy atoms of the first row in the periodic table in ion-atom collisions is needed in designing and operating controlled thermonuclear fusion devices based on confined hot plasma. They are also important in modeling the ionic structure of interstellar media. Steigman [1] suggested that the observed large disparity in abundance between  $C^{2+}$  and  $C^+$  ions in certain regions of the interstellar medium [2] might be due to rapid charge-transfer reactions, i.e.,



However, McCarroll and Valiron [3] estimated the transition probability on the basis of the Landau-Zener formula to be of the order of  $10^{-5}$  for thermal collisions and concluded that the above reaction is unlikely to be of importance as an efficient means of converting  $C^{2+}$  to  $C^+$  ions in an astrophysical environment. Butler *et al.* [4] studied radiative charge-transfer processes below 100 000 K, and found that the rate coefficient shows a weak temperature dependence and varies from  $1.58 \times 10^{-14}$  cm<sup>3</sup>/s at 10 K to  $2.44 \times 10^{-14}$  cm<sup>3</sup>/s at 100 000 K. Butler *et al.* [5] also calculated the capture cross section by using a quantum-mechanical method to obtain the rate coefficient at temperatures below  $5 \times 10^4$  K and found that the process is slow with a rate coefficient of the order of less than  $10^{-11}$  cm<sup>3</sup>/s. Heil *et al.* [6] calculated the capture cross section below a collision energy of 8.1 eV by using a full quantal approach with the three lowest  $^2\Sigma^+$  molecular states. They found that their calculated charge-transfer cross sections agree within the ex-

perimental uncertainty with measured values by Phaneuf [7]. At higher collision energies, Eichler *et al.* [8] calculated charge-transfer cross sections of the above process for collision energies from 40 to 1000 keV by using the Oppenheimer-Brinkman-Kramers approximation and found good agreement with the experimental data at higher energies reported by Goffe *et al.* [9].

On the experimental side, measurements were carried out in the range of 41.7 eV to 175 keV [7,9–11]. Tawara *et al.* [12] compiled the measured cross sections, and by using the procedure based on the Chebyshev fitting, combining the experimental and theoretical results, Janev *et al.* [13] tabulated cross sections for the  $1-2 \times 10^5$  eV energy region. However, to the best of our knowledge, no charge-transfer calculations based on rigorous *ab initio* studies for the process  $C^{2+} + H(^2S) \rightarrow C^+ + H^+$  have been carried out in the low-keV region of energy.

In this paper, we perform a study of charge transfer in the above process by using a molecular orbital (MO) expansion method within a semiclassical framework and have examined the final distribution of  $C^+$  ionic states. Furthermore, there has been some experimental controversy as to the existence of a bound state of the  $CH^{2+}$  ion [14], and our high-precision *ab initio* calculations are expected to shed some light on this long-standing problem.

## II. THEORETICAL MODEL

The present approach employed is the semiclassical impact parameter method based on a molecular orbital expansion. This method has been applied successfully to many systems, and details are given elsewhere [15]. Therefore, we provide only a brief summary here with some relevant information specifically needed for the present study.

TABLE I. Number of reference configurations,  $N_{\text{ref}}$ , and number of roots,  $N_{\text{root}}$ , treated in each irreducible representation and the corresponding number of generated ( $N_{\text{tot}}$ ) and selected ( $N_{\text{sel}}$ ) symmetry-adapted functions for a threshold of  $(1.5 \times 10^{-6})E_H$  at an internuclear distance of  $2.0a_0$ .

State	$N_{\text{ref}}/N_{\text{root}}$	$N_{\text{tot}}$	$N_{\text{sel}}$
$^2A_1$	82/7	497 401	12 015
$^2B_1$	38/4	331 611	7716
$^2A_2$	29/3	286 539	6487

### A. Molecular states and couplings

The adiabatic potential curves of  $\text{CH}^{2+}$  are obtained by employing the *ab initio* multireference single- and double-excitation configuration interaction (MRD-CI) method [16], with configuration selection at a selection threshold of  $(1.5 \times 10^{-6})E_H$  (energy in hartrees) and energy extrapolation using the Table CI algorithm [17]. All electrons, not only the valence ones, are included in the present CI calculation. The nonadiabatic coupling elements are calculated by using a finite-difference method [18]. In the calculation, the *s,p* basis set that we use for carbon atom is similar to the ‘‘basis set *F*’’ in Ref. [19] except that the most diffuse *p* function with exponent 0.008 has been deleted. Together with three *d* and one *f* polarization functions [20], the final basis set for carbon atom is  $(13s8p3d1f)$ , contracted to  $[8s6p3d1f]$ . The  $(10s4p1d)/[6s4p1d]$  contracted basis set of Ref. [21] is used for the hydrogen atom. Further details of our *ab initio* MRD-CI calculations are listed in Table I.

### B. Collision dynamics

A semiclassical MO expansion method with a straight-line trajectory of the incident ion was employed to study the collision dynamics below 1 keV [15]. In this approach, the relative motion of heavy particles is treated classically, while electronic motion is treated quantum mechanically. The total scattering wave function was expanded in terms of products of a molecular electronic state and atomic-type electron translation factors (ETF’s), in which the inclusion of the ETF satisfies the correct scattering boundary condition. Substituting the total wave function into the time-dependent Schrödinger equation and retaining the ETF correction up to first order in the relative velocity between the collision partners, we obtain a set of first-order coupled equations in time *t*. Transitions between the molecular states are driven by nonadiabatic couplings. By solving the coupled equations numerically, we obtain the scattering amplitudes for transitions: the square of the amplitude gives the transition probability, and integration of the probability over the impact parameter gives the cross section. Up to nine molecular states are included in the dynamical calculations as shown in Fig. 1, separating to  $[\text{H}+\text{C}^{2+}(^1S)](3^2\Sigma^+)$  as the initial channel and  $[\text{H}^++\text{C}^+(^2P)](1^2\Sigma^-, 3^2\Pi)$ ,  $[\text{H}^++\text{C}^+(^2S)](4^2\Sigma^+)$ ,  $[\text{H}^++\text{C}^+(^2D)](2^2\Sigma^+, 2^2\Pi, 1^2\Delta)$  and  $[\text{H}^++\text{C}^+(^2P)](1^2\Sigma^+, 1^2\Pi)$  for charge-transfer channels. In this energy range, the contribution from the  $\Delta$  state is normally expected to be weak, but it was included in addition to some higher levels to check the convergence of the

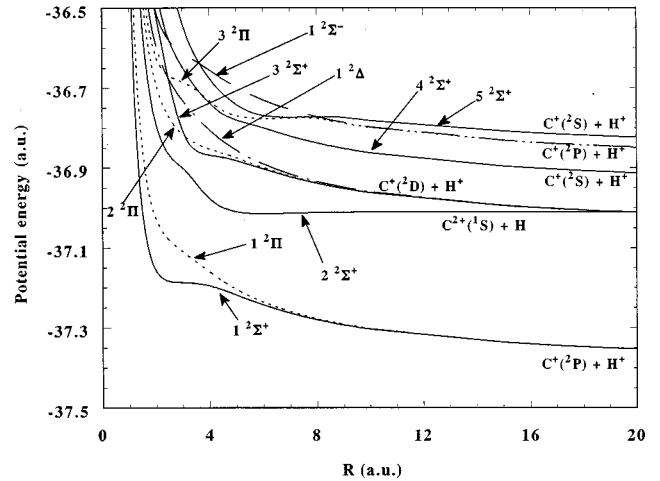


FIG. 1. Ten lowest adiabatic potentials of the doublet  $\text{CH}^{2+}$  system. The solid line represents  $\Sigma^+$  states, the dashed line for  $\Pi$  states, and the dot-dashed line for  $\Delta$  states. The long-dashed line is for the  $\Sigma^-$  state. Corresponding asymptotic atomic states are included in the figure.

cross sections in the present calculation. A detailed discussion of these states is given below.

## III. RESULTS

### A. Possible presence of a bound state of $\text{CH}^{2+}$

The calculated adiabatic potentials are shown in Fig. 1 [and also Figs. 2(a) and 2(b) for limited *R* regions where the potential minima are observed] from the lowest level to a few excited manifolds, and the numerical results for the  $1^2\Sigma^+$  and  $2^2\Sigma^+$  states are given in Table II. Wetzel *et al.* [14] performed experimental measurements, in combination with *ab initio* electronic structure calculations, in order to examine the possibility of forming a bound state in  $\text{CH}^{2+}$  ions. Their attempt was designed to detect long-lived  $\text{CH}^{2+}$  in multiple-electron impact ionization processes, but did not find any evidence for the existence of stable  $\text{CH}^{2+}$  ions. Their computation also supports the measurement suggesting that all ground and excited states of the  $\text{CH}^{2+}$  ion are repulsive and, hence, that no long-lived bound state exists. Our high-precision MRD-CI calculation also indicates that there is *no* minimum in the  $1^2\Sigma^+$  state of  $\text{CH}^{2+}$  at any *R* region. There is a minimum which is located at about  $R=6.0a_0$  for the  $2^2\Sigma^+$  potential, however, with a depth of about 0.14 eV based on the present calculated potential. A few vibrational levels can be held by this potential well. The curve of the  $2^2\Sigma^+$  state of  $\text{CH}^{2+}$  is found to be very flat in the region near the minimum, and the lowest level lies only about  $180\text{ cm}^{-1}$  higher.

This is understandable since in the region from  $5.0a_0$  to  $19.0a_0$ , the  $2^2\Sigma^+$  state corresponds asymptotically to the  $\text{C}^{2+}$  ion and H atom. At such large internuclear distances, the interaction between the  $\text{C}^{2+}$  ion and H atom is mainly attractive due to the long-range polarization interaction. It is also found that the widths (inverse of the lifetime) of the first and second vibrational levels of the  $2^2\Sigma^+$  state are in the order of only  $10^{-7}$  and  $10^{-6}\text{ cm}^{-1}$ , respectively, so that the predissociation of the  $2^2\Sigma^+$  state via  $1^2\Sigma^+$  is highly unlikely.

TABLE II. Numerical data of adiabatic potentials for  $1\ ^2\Sigma^+$  and  $2\ ^2\Sigma^+$  states around minimum locations.

$1\ ^2\Sigma^+$		$2\ ^2\Sigma^+$	
$R$ (a.u.)	Energy (a.u.)	$R$ (a.u.)	Energy (a.u.)
1.00	-36.311 31	3.00	-36.901 19
1.20	-36.724 15	3.05	-36.904 10
1.30	-36.851 53	3.10	-36.907 19
1.40	-36.944 91	3.15	-36.910 48
1.50	-37.013 33	3.20	-36.913 97
1.60	-37.063 34	3.25	-36.917 64
1.70	-37.099 80	3.30	-36.921 53
1.80	-37.126 21	3.35	-36.925 59
1.90	-37.145 20	3.40	-36.929 77
2.05	-37.163 91	3.60	-36.946 99
2.20	-37.174 89	3.80	-36.963 11
2.40	-37.182 49	4.00	-36.976 78
2.60	-37.185 71	4.05	-36.979 76
2.80	-37.186 99	4.10	-36.982 56
3.00	-37.187 52	4.15	-36.985 18
3.05	-37.187 66	4.20	-36.987 68
3.10	-37.187 81	4.25	-36.990 02
3.15	-37.187 93	4.30	-36.992 20
3.20	-37.188 09	4.35	-36.994 24
3.25	-37.188 23	4.45	-36.997 89
3.30	-37.188 42	4.50	-36.999 49
3.35	-37.188 69	4.55	-37.000 97
3.40	-37.189 00	4.60	-37.002 37
3.60	-37.190 55	4.80	-37.007 01
3.80	-37.192 83	5.00	-37.010 16
4.00	-37.195 91	5.20	-37.012 23
4.05	-37.196 82	5.40	-37.013 48
4.10	-37.197 74	5.60	-37.014 28
4.15	-37.198 69	5.80	-37.014 60
4.20	-37.199 72	6.00	-37.014 69
4.25	-37.200 73	6.50	-37.014 18
4.30	-37.201 80	7.00	-37.013 33
4.35	-37.202 91	7.50	-37.012 59
4.40	-37.204 04	8.00	-37.011 87
4.45	-37.205 21	8.20	-37.011 65
4.50	-37.206 38	8.40	-37.011 50
4.55	-37.207 54	8.60	-37.011 27
4.60	-37.208 79	8.80	-37.011 17
4.80	-37.213 81	9.00	-37.011 01
5.00	-37.219 01	9.20	-37.010 89
5.20	-37.224 22	9.40	-37.010 78
5.40	-37.229 39	9.60	-37.010 61
5.60	-37.234 44	9.80	-37.010 53
5.80	-37.239 31	10.00	-37.010 45
6.00	-37.243 99		

For a further check, we have carried out more elaborate calculations for the  $2\ ^2\Sigma^+$  state using the same basis set as given above, but keeping the  $1s$  orbital of carbon frozen. We have also calculated this state by using another (*cc-pVQZ*) basis set [20] ( $1s$  orbital of carbon is again frozen). In both cases, a possible error caused by the energy extrapolation is removed. The depths of the well obtained are 0.15 and 0.136

eV, respectively, which are consistent with our original result.

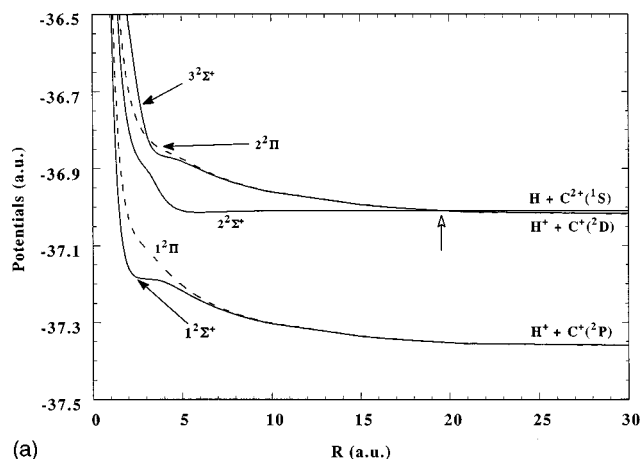
Wetzel *et al.* [14], on the contrary, have reported that no such bound state of CH<sup>2+</sup> was found. Our calculations are believed to be more accurate than those of Wetzel *et al.*, however, and the mesh used in the *ab initio* calculations of Wetzel *et al.* [14] may have been too large to find this minimum. Some experimental investigations [22,23] have also suggested the possibility of the existence of a bound state for CH<sup>2+</sup>, but others have reported the contrary [14,24]. Similar divergences among various theoretical results [6,14,24,25] also exist. Based on our calculations and the arguments above, we feel there is a good chance that the  $2\ ^2\Sigma^+$  state of CH<sup>2+</sup> should be a metastable state. It should be pointed out that our present calculations are not specifically designed to calculate accurate vibrational levels for such shallow states, however, and so further detailed calculations for the  $2\ ^2\Sigma^+$  state of CH<sup>2+</sup> with still higher accuracy would be needed to carefully describe the spectroscopic constants for this state.

## B. Charge-transfer dynamics from the ground C<sup>2+</sup> ions

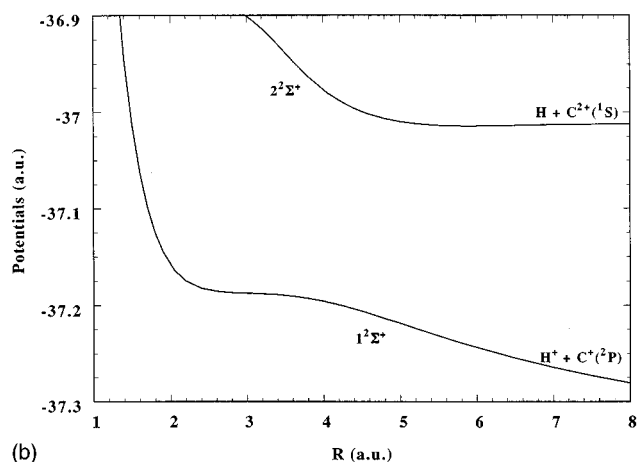
In the present study, we have carried out cross section calculations by taking couplings of three states ( $1\ ^2\Sigma^+$ ,  $2\ ^2\Sigma^+$ , and  $3\ ^2\Sigma^+$ ), four states (three states plus  $1\ ^2\Pi$ ), five states (three states plus  $1\ ^2\Pi$  and  $2\ ^2\Pi$ ), seven states (five states plus  $1\ ^2\Delta$  and  $4\ ^2\Sigma^+$ ), and nine states (seven states plus  $1\ ^2\Sigma^-$  and  $3\ ^2\Pi$ ) into account (as shown in Fig. 1) to ensure the convergence of the result. We have found that the present seven-state result converges reasonably well within a few percent, and hence, our discussion below is mostly based on the five- or seven-state calculation. The  $^2\Delta$  state contribution is normally found to be weak in the energy region studied, since the transition to the  $^2\Delta$  state from the initial incoming  $3\ ^2\Sigma^+$  state requires a change of  $\Delta\Lambda=2$ , i.e., a two-step process, where  $\Lambda$  is the absolute value of the projection of angular momentum along the molecular axis. However, in the present case this situation may be slightly different since the  $^2\Delta$  state is nearly degenerate with the  $2\ ^2\Sigma^+$  and  $2\ ^2\Pi$  states in the large- $R$  region (see Fig. 1) which also couple strongly with the initial channel, and hence a careful examination of the role of the  $^2\Delta$  state is desirable.

### 1. Adiabatic potentials

Five adiabatic potential curves which are dominant channels in the present calculations are displayed in Fig. 2(a), and the  $1\ ^2\Sigma^+$  and  $2\ ^2\Sigma^+$  potentials at small  $R$  where they have a minimum are illustrated in Fig. 2(b). Further, asymptotic energy differences among states and corresponding asymptotic atomic states are shown in Table III. There is a strong avoided crossing between the  $2\ ^2\Sigma^+$  and  $3\ ^2\Sigma^+$  states at  $R=19.4$  a.u. (with energy separation  $<8\times 10^{-5}$  a.u.), and the corresponding potentials and coupling matrix elements involving the  $2\ ^2\Sigma^+$  and  $3\ ^2\Sigma^+$  states abruptly exchange places. There is also another moderate avoided crossing near  $R=3$  a.u. between these states. The present outer crossing may be compared with the findings of earlier work by McCarron and Valiron [3], who calculated the molecular adiabatic potentials by using a model potential approach for the C atomic core and found that the  $2\ ^2\Sigma^+$  and  $3\ ^2\Sigma^+$  had an



(a)



(b)

FIG. 2. (a) Three  $2^2\Sigma^+$  and two  $2^2\Pi$  molecular states of  $\text{CH}_2^+$  which were included in the present dynamical calculations. The open arrow indicates the position of the avoided crossing between  $2^2\Sigma^+$  and  $3^2\Sigma^+$  at  $R=19.4$  a.u. (b)  $1^2\Sigma^+$  and  $2^2\Sigma^+$  potentials near the region where they have a minimum.

avoided crossing at 18.3 a.u., and that of Heil *et al.* [6], who carried out CI calculations for the adiabatic potentials and found crossings at  $R\sim 3$  and 24 a.u. However, Heil *et al.* in their cross section calculation at low-eV energies assumed that the outermost avoided crossing had no effect on the reaction considered and treated it as such. In contrast to their assumption, we assumed that the  $2^2\Sigma^+$  and  $3^2\Sigma^+$  potentials cross at  $R=19.4$  a.u. and constructed the so-called ‘‘diabatic states’’ as  $2^2\Sigma_d^+$  and  $3^2\Sigma_d^+$  by switching the potentials and corresponding coupling matrix elements

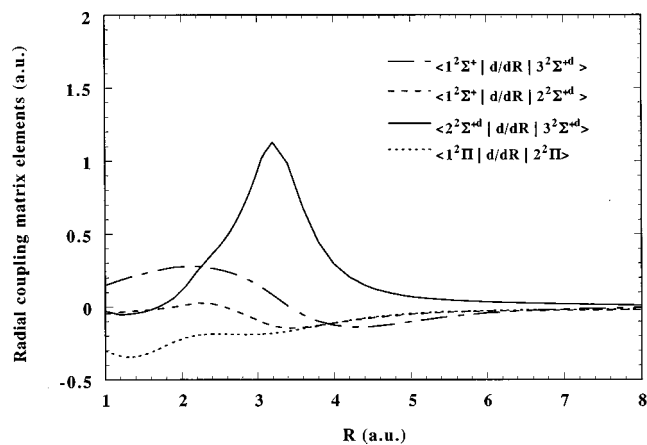


FIG. 3. Representative radial coupling matrix elements. The superscript  $d$  denotes ‘‘diabatic’’ states.

involving the  $2^2\Sigma^+$  and  $3^2\Sigma^+$  states at  $R<19.4$  a.u. and  $R>19.4$  a.u. Note that the meaning of ‘‘diabatic’’ used here is different from the one used for eliminating the first-order derivatives with respect to  $R$  in the Schrödinger equation. Now the incoming channel is  $3^2\Sigma_d^+$ . In the present calculation, we include only a limited number of states lying higher than the  $3^2\Sigma^+$  state, and therefore the cross section for higher levels is considered as a reference. Hence we limit ourselves to collision dynamics for low-keV energies.

## 2. Nonadiabatic coupling matrix elements

Representative radial and rotational coupling matrix elements among these dominant five states are shown in Figs. 3 and 4, respectively. In Fig. 3, we can see a sharp peak in the radial coupling matrix element between the  $2^2\Sigma_d^+$  and  $3^2\Sigma_d^+$  states at  $R\sim 3.2$  a.u. where an avoided crossing occurs. The rotational coupling matrix elements between  $2^2\Sigma_d^+$  and  $2^2\Pi$ , and  $2^2\Pi$  and  $1^2\Delta$  approach a constant value beyond  $R\sim 6$  a.u. and so does the rotational coupling matrix element between the  $1^2\Sigma^+$  and  $1^2\Pi$  states because of the degeneracy of states. From Figs. 2–4, we might expect an efficient flux mixing to occur among  $2^2\Sigma_d^+$ ,  $3^2\Sigma_d^+$ ,  $2^2\Pi$ , and  $1^2\Delta$  in a rather complex manner and also that a transition via the route of  $3^2\Sigma_d^+\rightarrow 2^2\Pi\rightarrow 2^2\Sigma_d^+\rightarrow 2^2\Pi\rightarrow 3^2\Sigma_d^+$ , which eventually reduces charge transfer, is likely to proceed.

## 3. Total charge-transfer cross sections

In Fig. 5, charge-transfer cross sections for the process (1) obtained by using the seven-state calculations are displayed

TABLE III. Doublet states and corresponding asymptotic energies as well as atomic designations.

Molecular states	Asymptotic relative energies <sup>a</sup> ( $\text{cm}^{-1}$ )	Asymptotic atomic states
$1^2\Sigma^+, 1^2\Pi$	0	$\text{H}^+ + \text{C}^+(2s^2 2p^2: ^2P)$
$2^2\Sigma^+, 2^2\Pi, 1^2\Delta$	74 931	$\text{H}^+ + \text{C}^+(2s 2p^2: ^2D)$
$3^2\Sigma^+$	86 980	$\text{H} + \text{C}^{2+}(2s^2: ^1S)$
$4^2\Sigma^+$	96 494	$\text{H}^+ + \text{C}^+(2s 2p^2: ^2S)$
$1^2\Sigma^-, 3^2\Pi$	110 625	$\text{H}^+ + \text{C}^+(2s 2p^2: ^2P)$
$5^2\Sigma^+$	116 538	$\text{H}^+ + \text{C}^+(2s^2 3s: ^2S)$

<sup>a</sup>The relative energies listed correspond to the differences between the lowest  $J$  levels of the upper and lower electronic states.

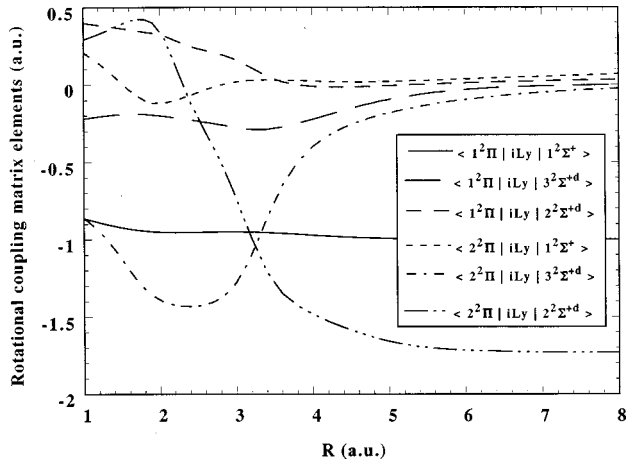


FIG. 4. Representative rotational coupling matrix elements. The superscript  $d$  denotes “diabatic” states.

together with experimental data of Tawara *et al.* [12] and theoretical results from Heil *et al.* [6] for low energies. Also, the Chebyshev curve fit to available experimental and theoretical results by Janev *et al.* [13] is included for a reference. Our semiclassical calculations show the overall trends in energy dependence, which agree well with experiment, although the magnitude of the present cross sections is found to be larger for all energies; the difference increases with energy. The experiment claims an overall accuracy of 20% in this energy range [13]. By way of comparison, for example, the present calculation differs nearly by 50% at the highest energy studied. At low energies, our result seems to tie in well with the quantum-mechanical result of Heil *et al.*, whose cross sections back up at much lower energy below 5 eV. The small structures seen in the intermediate-energy region are due to a multichannel interference effect.

The present results converge reasonably well with respect to basis sets used in the calculation; the results of the seven-state calculation are found to converge within 3% of the nine-state calculation, and that of the five-state calculation is within 8% of the seven-state calculation at the highest energy studied. The three- and four-state calculations are not suffi-

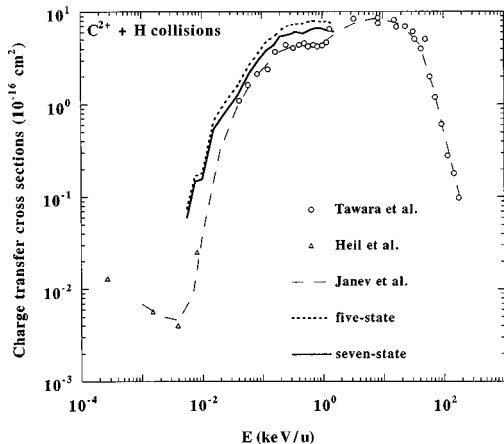
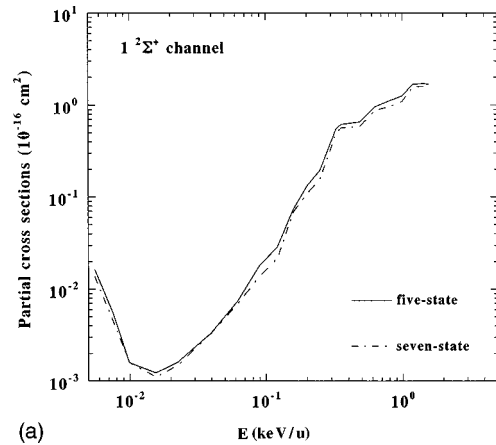
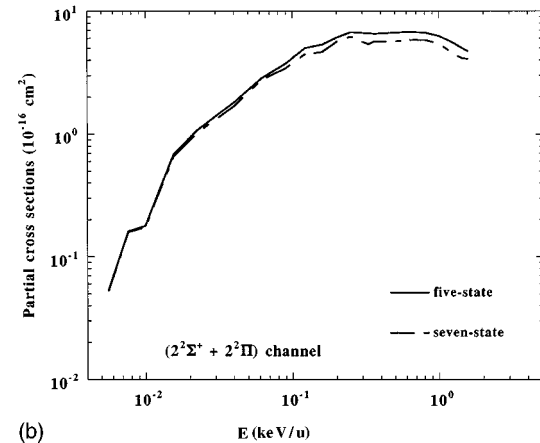


FIG. 5. Charge-transfer cross sections: solid line, seven-state result; dotted line, five-state result; triangle, Ref. [5]. Experiment: circle (Ref. [11]), dashed line (Ref. [7]).



(a)



(b)

FIG. 6. Partial charge-transfer cross sections of (a)  $1^2\Sigma^+$  and (b)  $2^2\Sigma^+$  and  $2^2\Pi$  by using five- and seven-state calculations.

cient, but they describe most of the essential dynamics reasonably well. At low energies, all calculations using the different basis sizes give nearly identical results. As the collision energy increases, the agreement among different basis sets becomes poorer, but again, seven- and nine-state calculations are regarded as converged. It may be worthwhile noting that the addition of the  $1^2\Delta$  state to the five-state basis set is found to be rather important since the  $1^2\Delta$  state plays the role of a flux reservoir, and on the outgoing part of the collision, it returns the flux back to the initial channel through  $2^2\Pi$ , hence resulting in a decrease of the cross section.

#### 4. Partial charge-transfer cross sections

In Figs. 6(a) and 6(b), partial cross sections calculated by the five- and seven-state treatments are illustrated. As seen in Fig. 6(a), the partial cross sections of  $1^2\Sigma^+$  (and  $1^2\Pi$ , not shown) which correspond to  $[H^+ + C^+(2s^22p^1)]$  do not change significantly from five to seven (nine) states, indicating that these partial cross sections are not affected much by inclusion of higher MO's. The partial cross sections of  $2^2\Sigma^+$   $[H^+ + C^+(2s^22p^2;^2D)]$  do not change in three- and four-state calculations. However, in the five-state calculation, the partial cross section of  $2^2\Sigma^+$  is reduced considerably by inclusion of  $2^2\Pi$ , and the cross section of  $2^2\Pi$  is compa-

TABLE IV. Rate coefficients for the charge-transfer reaction.

Temperature (K)	Rate coefficients (cm <sup>3</sup> /s)			
	Present	Ref. [13]	Ref. [5]	Ref. [4] <sup>a</sup>
100				$1.50 \times 10^{-14}$
1000				$1.23 \times 10^{-14}$
5000			$1.0 \times 10^{-12}$	
10 000			$1.0 \times 10^{-12}$	$1.71 \times 10^{-14}$
20 000	$4.4 \times 10^{-12}$	$1.5 \times 10^{-12}$	$1.35 \times 10^{-12}$	
50 000	$5.4 \times 10^{-11}$	$2.3 \times 10^{-11}$	$1.49 \times 10^{-11}$	
100 000	$2.2 \times 10^{-10}$	$1.4 \times 10^{-10}$		$2.44 \times 10^{-14}$
500 000	$2.4 \times 10^{-9}$	$2.0 \times 10^{-9}$		

<sup>a</sup>Radiative charge-transfer reaction rates. All other rates are for nonradiative charge transfer.

able to that of  $2^2\Sigma^+$ ; i.e., the flux is shared by both degenerate states. Consequently, the total cross sections in the five-state calculation become larger than those of three- and four-state calculations. In the five-state calculation, the major contributing channel is  $2^2\Pi$  [ $H^+ + C^+(2s^1 2p^2)$ ], closely followed by the  $2^2\Sigma^+$  [ $H^+ + C^+(2s^1 2p^2)$ ] state. Consequently, at low-keV energies, the outgoing  $C^+$  ions will be mostly  $C^+(2s^1 2p^2; ^2D)$ . Once the  $1^2\Delta$  state is added to the five-state calculation, making it the seven-state calculation, it plays the role of a reservoir of the flux from  $2^2\Pi$  in the incoming part of the collision, and the flux returns to the initial channel at the outgoing part of the collision through a two-step  $1^2\Delta \rightarrow 2^2\Pi \rightarrow 3^2\Sigma^+$  transition, thus reducing the magnitude of the charge-transfer cross section. Transitions to higher MO's, corresponding to  $1^2\Sigma^-$  and  $3^2\Pi$  [ $H^+ + C^+(2s^1 2p^2; ^2P)$ ] states, are found to be small within the model at the highest energy studied, but the basis size we employed is not adequate to assess the magnitude of this cross section. Calculations by Heil *et al.* [6] at energies below a few eV suggested that the outgoing  $C^+$  ions are in the  $C^+(2s^2 2p^1; ^2P)$  ground state at low energies, but the  $C^+(2s 2p^2; ^2D)$  product ions begin to dominate above 4 eV. In view of the fact that the present cross sections agree well on the very-low-energy side, it is justifiable to employ three  $^2\Sigma^+$  states for much lower energies.

### C. Rate coefficients

The rate coefficients based on the present theory are provided in Table IV along with those calculations based on the cross sections by the fitting procedure of Janev *et al.* [13] and by Butler *et al.* [5]. Also, we have included those for radiative charge transfer by Butler *et al.* [4]. Note that the present calculations have been carried out by focusing on intermediate- and high-energy collisions, and hence the present results for the low end of collision energies may not be of high accuracy, as is apparent from the discussion above. Therefore, our values tabulated should be considered to be tentative, although our results should provide a correct order of magnitude. As reflected from the present cross section, our rate coefficients are larger by 50% at all temperatures compared to those by Janev *et al.* The rate coefficients by Butler *et al.* agree reasonably well with those of Janev *et al.* where their temperatures overlap. The rate coefficients due to radiative charge transfer are much smaller than those

of nonradiative charge transfer, and hence the radiative process is considered to be unimportant above a few 1000 K.

## IV. CONCLUSION

We have calculated several adiabatic states of  $CH^{2+}$  by using a highly accurate CI method. The present *ab initio* calculations do not find any minimum in the  $1^2\Sigma^+$  potential, but do find a very shallow well at  $R=6.0$  a.u. for the  $2^2\Sigma^+$  state, suggesting that a bound electronic state might exist. However, further, more accurate calculations as well as a more elaborate experimental search for this electronic state are desirable before making such a conclusion. Single-charge transfer cross sections in collisions of  $C^{2+}$  ions with H atoms were calculated at low-keV collision energies by using the semiclassical impact parameter method based on a molecular orbital expansion with three, four, five, seven, and nine MO states. The outgoing  $C^+$  ions are mostly of the  $C^+(2s 2p^2; ^2D)$  state. The present results show good overall agreement in shape with experiment, but the magnitude is found to be slightly larger. The corresponding rate coefficients are also in a reasonable agreement with other theories obtained for astrophysical and fusion research. We also have found that the contribution from the  $1^2\Delta$  state is important for the flux redistribution, thus reducing the size of the charge-transfer cross section.

## ACKNOWLEDGMENTS

This work was supported in part by the Deutsche Forschungsgemeinschaft in the form of a Forschergruppe and Grant No. Bu 450/7-1. The financial support of the Fonds der Chemischen Industrie is also hereby gratefully acknowledged. We thank Dr. Yan Li for a useful discussion and for calculating the widths and lifetime of the vibrational levels of the  $2^2\Sigma^+$  state. M.K. also acknowledges financial support from the National Science Foundation through the Institute of Theoretical Atomic and Molecular Physics (ITAMP), Harvard-Smithsonian Center for Astrophysics, when this project was initiated. The authors thank Professor Dalgarno for a useful discussion.

- [1] G. Steigman, *Astrophys. J., Lett. Ed.* **195**, L39 (1975).
- [2] J. B. Rogerson, D. G. York, J. F. Drake, E. B. Jenkin, D. C. Morton, and L. Spitzer, *Astrophys. J., Lett. Ed.* **181**, L110 (1973).
- [3] R. McCarroll and P. Valiron, *Astron. Astrophys.* **44**, 465 (1975).
- [4] S. E. Butler, S. L. Guberman, and A. Dalgarno, *Phys. Rev. A* **16**, 500 (1977).
- [5] S. E. Butler, T. G. Heil, and A. Dalgarno, *Astrophys. J.* **241**, 442 (1980).
- [6] T. G. Heil, S. Butler, and A. Dalgarno, *Phys. Rev. A* **23**, 2833 (1983).
- [7] R. Phaneuf, *Phys. Rev. A* **24**, 1138 (1981).
- [8] J. K. M. Eichler, A. Tsuji, and T. Ishihara, *Phys. Rev. A* **23**, 2833 (1980).
- [9] T. V. Goffe, M. B. Sha, and H. B. Gilbody, *J. Phys. B* **12**, 3763 (1979).
- [10] L. D. Gardner, J. E. Bayfield, P. M. Koch, I. A. Sellin, D. J. Pegg, R. S. Peterson, and D. H. Crandall, *Phys. Rev. A* **21**, 1387 (1980).
- [11] R. Phaneuf, F. W. Meyer, and R. H. McKnight, *Phys. Rev. A* **17**, 534 (1978).
- [12] H. Tawara, T. Kato, and Y. Nakai, *At. Data Nucl. Data Tables* **32**, 235 (1985).
- [13] R. K. Janev, R. A. Phaneuf, and H. T. Hunter, *At. Data Nucl. Data Tables* **40**, 249 (1988).
- [14] T. L. Wetzel, R. F. Welton, E. W. Thomas, R. F. Borkman, and T. F. Moran, *J. Phys. B* **26**, 49 (1993).
- [15] M. Kimura and N. F. Lane, in *Advances in Atomic, Molecular and Optical Physics*, edited by D. R. Bates and B. Bederson (Academic, New York, 1989), Vol. 26, p. 79.
- [16] R. J. Buenker and S. D. Peyerimhoff, *Theor. Chim. Acta* **35**, 33 (1974); **39**, 217 (1975); R. J. Buenker, *Int. J. Quantum Chem.* **29**, 435 (1986).
- [17] R. J. Buenker, in *Proceedings of the Workshop on Quantum Chemistry and Molecular Physics*, Wollongong, Australia, 1980, edited by P. G. Burton (University Press, Wollongong, Australia, 1980); in *Studies in Physical and Theoretical Chemistry*, edited by R. Carbo, Current Aspects of Quantum Chemistry Vol. 21 (Elsevier, Amsterdam, 1981), p. 17; R. J. Buenker and R. A. Phillips, *J. Mol. Struct.: THEOCHEM* **123**, 291 (1985).
- [18] G. Hirsch, P. J. Bruna, R. J. Buenker, and S. D. Peyerimhoff, *Chem. Phys.* **45**, 335 (1980).
- [19] M. Larsson and P. E. M. Siegbahn, *J. Chem. Phys.* **79**, 2270 (1983).
- [20] T. H. Dunning, Jr., *J. Chem. Phys.* **90**, 1007 (1989) (one *g* function for *C* and one *f* function for *H* are deleted).
- [21] M. Jaszunski, A. Rizzo, and D. L. Yeager, *J. Chem. Phys.* **89**, 3063 (1988).
- [22] T. Ast, C. J. Porter, C. J. Proctor, and J. H. Beynon, *Chem. Phys. Lett.* **78**, 439 (1981).
- [23] D. Mathur and C. Badrinathan, *J. Phys. B* **20**, 1517 (1989).
- [24] W. Koch, B. Liu, T. Weiske, C. B. Lebrilla, T. Drewello, and H. Schwarz, *Chem. Phys. Lett.* **142**, 147 (1987).
- [25] R. W. Wetmore, R. K. Boyd, and R. J. Le Roy, *Chem. Phys.* **89**, 329 (1984).